

SERI/TP-255-2018
UC Category: 59c
DE83011984

Advanced Phase-Change Storage: Analysis of Materials and Configurations

Craig Christensen

June 1983

To be presented at the ASES
PASSIVE 83 Conference
Glorieta, New Mexico
7-9 September 1983

Prepared under Task No. 1462.53
WPA No. 420

Solar Energy Research Institute

A Division of Midwest Research Institute

1617 Cole Boulevard
Golden, Colorado 80401

Prepared for the
U.S. Department of Energy
Contract No. EG-77-C-01-4042

Printed in the United States of America
Available from:
National Technical Information Service
U.S. Department of Commerce
5285 Port Royal Road
Springfield, VA 22161
Price:
Microfiche \$4.50
Printed Copy \$7.00

NOTICE

This report was prepared as an account of work sponsored by the United States Government. Neither the United States nor the United States Department of Energy, nor any of their employees, nor any of their contractors, subcontractors, or their employees, makes any warranty, express or implied, or assumes any legal liability or responsibility for the accuracy, completeness or usefulness of any information, apparatus, product or process disclosed, or represents that its use would not infringe privately owned rights.

**ADVANCED PHASE-CHANGE STORAGE FOR PASSIVE SOLAR HEATING:
ANALYSIS OF MATERIALS AND CONFIGURATIONS**

Craig B. Christensen

Solar Energy Research Institute
1617 Cole Boulevard
Golden, Colorado 80401

ABSTRACT

In this paper we discuss the performance of phase-change materials (PCMs) as thermal storage in passive solar heating systems. We discuss factors, other than material properties, that affect storage performance and optimization. We also briefly describe solid-state phase-change materials (SS PCMs) and list typical material properties. We give results from a parametric analysis of PCM Trombe walls, and discuss the factors that limit performance. We present configurations for enhanced PCM performance, and give simulation results for an idealized case.

1. INTRODUCTION

The effectiveness of thermal storage in passive solar systems depends on a number of factors, the most obvious being the thermophysical properties of the storage material. Parametric analysis can identify optimum properties and sensitivities to suboptimum properties. However, such analysis is complicated by the number of properties (and system parameters) of interest and by the fact that the optima and sensitivities for a particular property depend on other properties and parameters that may have suboptimum values.

Storage effectiveness also depends on context; i.e., the details of the passive system and the building. For instance, the addition of highly insulated glazing to a passive system alters the effectiveness of the system (Trombe wall or direct gain) and is likely to alter the effectiveness of different storage materials. Similarly, increasing building insulation levels alter the seasonal heating load patterns and the daily load profiles and is likely to favor one storage material over another. For near-term applications it is reasonable to evaluate storage materials in the context of typical current passive solar systems and building types. For future applications, assumptions are not as well defined, and additional system and building types must be considered, but preliminary analysis of typical system and building types may serve as a point of departure. It should be emphasized, however, that a stated storage equivalence (e.g., a given PCM has four times the volumetric heat storage capacity of concrete) is situation specific. Such an equivalence is useful for comparison but is

not necessarily general and should not be interpreted as an absolute limit on performance for that material except in the situation evaluated. It may be useful to determine maximum theoretical performance as an idealized situation by placing an upper bound on performance for a particular class of materials.

To date, storage material performance in passive solar systems has been analyzed to predict overall system performance and storage component heat transfer. The system performance studies (1,2) have been based on computer simulations for a limited number of typical storage materials, solar systems, building types, and locations. The heat transfer studies (3,4) have been more detailed including optimization, but have been based on analytical solutions with simplified boundary conditions or numerical simulations with limited building models.

2. SOLID-STATE PHASE-CHANGE MATERIALS

A solid-state phase-change material is any material that absorbs or releases energy when changing from one solid phase to another solid phase. The Solar Energy Research Institute (SERI) has studied the properties of such materials for possible use as thermal storage in various solar applications. The organic SS PCMs, which we are now studying for passive solar applications, were first considered for use in the passive temperature control of earth satellites. Under National Aeronautical and Space Administration (NASA) sponsorship, numerous such SS PCMs were evaluated ten years ago (5). At SERI, we have extended the earlier NASA research and discovered organic solid solutions that lower the useful temperature range of SS PCMs to where the passive solar system designer would be interested (6).

The most promising materials are solid solutions of pentaerythritol ($C_5H_{12}O_4$), pentaglycerine ($C_5H_{12}O_3$), and neopentyl glycol ($C_5H_{12}O_2$). Solid-solution mixtures of these compounds can be tailored so they exhibit solid-to-solid phase transformations at any desired temperature within a range from less than $25^\circ C$ to $188^\circ C$. Table 1 lists some of the characteristics of the three compounds and an example of the solid solutions that are the focus of this work. From the table it is

Table 1. Comparison of Phase-Change Thermal Energy Storage Materials

Constituents	Latent Heat of Transition	Transition Temperature	Solid Material Density	Raw Materials Cost*
	kJ/kg (Btu/lb)	°C (°F)	kg/m ³ (lb/ft ³)	\$/kg (\$/lb)
Solid-State PCMs				
Pentaerythritol (PE)	269 (115.7)	188 (370)	1390 (86.7)	1.56 (0.71)
Pentaglycerine (PG)	139 (59.8)	89 (192)	1220 (76)	1.51 (0.73)
Neopentyl-glycol (NPG)	119 (51.2)	48 (118)	1060 (66)	1.30 (0.59)
Solid-solution mixture of 60% NPG plus 40% PG	76 (32.7)	25 (79)	1124 (70)	1.46 (0.66)
Solid-Liquid PCMs				
Sodium sulfate decahydrate	225 (96.8)	32 (90)	1464 (91)	0.10 (0.045)
Calcium chloride hexahydrate	190.8 (82.1)	27 (81)	1802 (112.5)	0.145 (0.066)

*Chemical Marketing Reporter, 223, No. 7, Schnell Publishing Co., New York, (14 Feb. 1983).

apparent that the latent heat of transformation is typically lower for SS PCMs with lower transition temperatures. Currently, we are investigating the reasons for this relationship in an effort to develop materials that do not suffer from reduced latent heats of transformation.

One of the concerns with using PCMs for thermal energy storage is the stability of the material and its retention of full, reversible latent heat of transformation after several thermal cycles. The solid-state phase-change process is quite different from the salt hydrate solid-to-liquid PCMs and is not expected to suffer any changes during cycling because there is so little migration of material in the solid even above the transformation temperature. Preliminary experiments support the contention that the SS PCMs are basically stable to thermal cycling.

Another common problem with PCMs is undercooling; i.e., when the PCM is cooled from above the transition temperature, the reverse transformation that liberates the stored heat occurs at a lower temperature than the forward transformation. This undercooling effect is particularly great in SS PCMs. Experiments have shown that the kinetics of the transformation can be changed by adding a nucleating agent that lowers the activation energy for the nucleation of the phase transformation. For instance, adding 0.1% fine graphite powder reduced the undercooling significantly, particularly at low heating and cooling rates. Further experiments are needed to determine minimum achievable undercooling at the lower heating and cooling rates typical of passive systems.

3. PARAMETRIC ANALYSIS OF PCM TROMBE WALLS

In this section, we give assumptions and results for a parametric analysis of PCM Trombe walls and discuss the factors that limit performance.

3.1 Assumptions

The properties of neopentyl glycol were used as a starting point for the parametric analysis. Thermal conductivity and the phase transformation temperature were varied as parameters to evaluate the performance for modified neopentyl glycol or other PCMs. Enthalpy of transformation, density, and specific heat were held constant at the nominal values of neopentyl glycol. In these preliminary analyses, we did not include the effect of undercooling.

Thermal analysis was based on simulations using the SERIRES computer code (7) and ersatz ETMY (8) weather data for Denver, Colo. The thermal network model for the building and the Trombe wall were solved by forward finite differencing with time steps of 6 min or less. Solar savings fractions were based on annual simulations with and without the Trombe wall.

Table 2 lists characteristics of the building model, which was based on the SERI test house, a single-story, three-bedroom house that has been extensively monitored (Class A). We determined a base annual heating load of 3430 kWh (11.7 X 10⁶ Btu) from a SERIRES simulation assuming an adiabatic south wall (for calculating solar savings fractions).

Table 2. Building Characteristics*

Floor area = 100 m ² (1080 ft ²)
Windows = double glazed
Ceiling = RSI 5.3 (R30)
Walls = RSI 1.9 (R11)
Crawlspace walls = RSI 3.3 (R19)
Infiltration = 0.5 ACH
Internal gains = 56,000 kJ/day (53,000 Btu/day)
Heating setpoint = 20°C (68°F)
Venting setpoint = 24.4°C (76°F)
Cooling setpoint = 25.6°C (78°F)

Table 3. Trombe Wall Characteristics

Area = 18.6 m ² (200 ft ²)
Glazing = double
Vent area = 3%
Concrete
Thermal conductivity = 1.31 W/m °C (0.7576 Btu/ft °F h)
Density = 2243 kg/m ³ (140 lb/ft ³)
Specific heat = 0.837 kJ/kg °C (0.2 Btu/lb °F)
Phase-change materials
Density = 1066 kg/m ³ (66.55 lb/ft ³)
Specific heat = 2.5 kJ/kg °C (0.5996 Btu/lb °F)
Heat of transformation = 121 kJ/kg (52.03 Btu/lb)

Table 3 lists characteristics of the Trombe wall. Thermal storage was modeled with multiple nodes to account for the effect of thermal conductivity and the resulting temperature gradients in the wall.

3.2 Results

Figure 1 shows the results of a series of simulations with the phase transformation temperature as a parameter and with a wall thickness of 5.1 cm (2.0 in.). For the nominal PCM thermal conductivity, the optimum phase transformation temperature is 29°C (84°F). For a PCM with thermal conductivity increased by a factor of five, the optimum transformation temperature is 27°C (80°F).

Figure 2 shows results with thermal conductivity as a parameter. For a transition temperature of

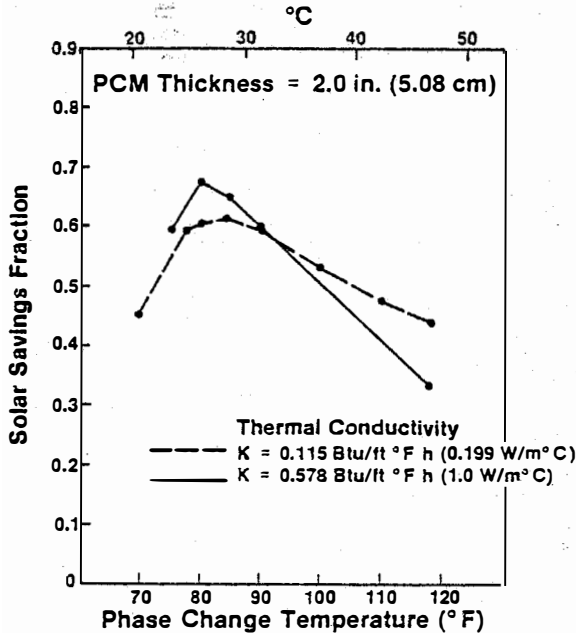


Fig. 1. Solar Savings Fraction as a Function of Phase-Change Temperature in a PCM Trombe Wall

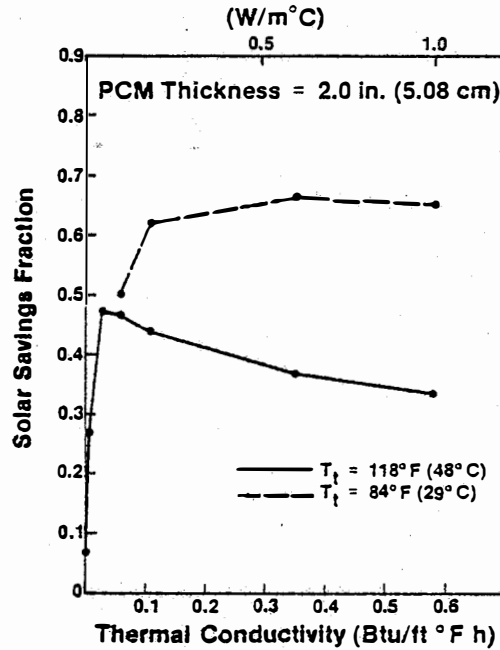


Fig. 2. Solar Savings Fraction as a Function of Thermal Conductivity in a PCM Trombe Wall

48°C (118°F), performance is optimized when the thermal conductivity is about 0.05 W/m °C (0.03 Btu/h ft °F) and declines rapidly for lower values. For a transition temperature of 29°C (84°F), performance is relatively insensitive to thermal conductivity, except for conductivity values below 0.17 W/m °C (0.1 Btu/h ft °F) where performance declines rapidly.

Figure 3 shows Trombe wall performance as a function of wall thickness for parameters listed in Table 4. Curve A gives results for an idealized PCM Trombe wall discussed in Sec. 3.3. Curve C gives results for a concrete Trombe wall for comparison. The remaining curves give results for PCM Trombe walls with various material properties.

For concrete Trombe walls, thickness is shown along the abscissa at the top of the graph. For the PCM walls, thickness is shown along the lower abscissa, which is scaled one-fourth the thickness of concrete.

3.3 Discussion of Results

The optimum phase transformation temperatures for PCM Trombe walls (Fig. 1) are caused by trade-offs between storage heat delivery rates and storage heat loss rates during the heating season. For transition temperatures below the optimum, performance is limited by heat delivery rates that are inadequate relative to hourly heating loads. For transition temperatures above the optimum, storage losses are increased owing to backlosses through the glazing and losses caused by unnecessary heating of the building.

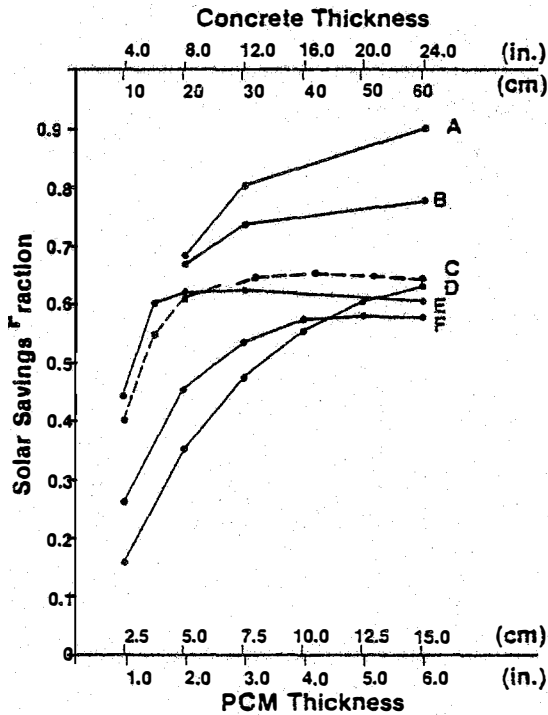


Fig. 3. Solar Savings Fraction as a Function of Trombe Wall Thickness for SS PCMs and Concrete. (See Table 4 for parameter values.)

The sensitivity to thermal conductivity for PCM Trombe walls (Fig. 2) depends on the phase transformation temperature. For a transition temperature of 29°C (84°F), the results indicate that performance will be near optimum if the thermal conductivity of the PCM is large enough so the interior surface temperature of the Trombe wall is near the transition temperature even when the phase transition boundary is near the center of the wall. For a phase transformation temperature of 48°C (118°F) and a large thermal conductivity, performance is low because: (1) during charging, heat is conducted to the interior surface and into the room at such a rate that less of the wall is heated up to the phase transformation temperature, and (2) once charged, the wall discharges and loses heat at an excessive rate. For a phase transformation temperature of 48°C (118°F) and a lower thermal conductivity, performance is somewhat improved. The improvement is limited because a trade-off exists between the discharge and heat loss rates and conduction of heat into the wall during charging.

Performance of PCM Trombe walls (Fig. 3) varies over a wide range depending on material properties. For case E, performance is approximately equivalent to the performance of a concrete Trombe wall four times as thick. For higher transition temperatures (cases D and F), performance is lower. In case B, transition temperature and thermal conductivity are optimized, and solar fractions are 10%-20% higher than solar fractions for a concrete Trombe wall. Note that the transi-

Table 4. Parameter Values for Fig. 3

Case*	Transfor- mation Temperature	Thermal Conduc- tivity	Heat- Transfer Coefficient
	°C (°F)	W/m °C (Btu/ ft °F h)	W/m ² °C (Btu/ ft ² °F h)
A	20.3 (68.5)	1728 (999)	567 (99.9)
B	27 (80)	1.00 (0.578)	8.29 (1.46)
C	Concrete	1.31 (0.758)	8.29 (1.46)
D	48 (118)	1.00 (0.578)	8.29 (1.46)
E	29 (84)	0.20 (0.115)	8.29 (1.46)
F	48 (118)	0.20 (0.115)	8.29 (1.46)

*All cases are for SS PCMs except for C.

tion temperature and thermal conductivity have been optimized for a 5-cm (2-in.) thick wall and that solar fractions for thicker walls may increase if these properties are optimized for those thicknesses.

PCM heat storage capacities are often quoted relative to concrete, assuming operation over a particular temperature range. A relative heat capacity implies an equivalent thickness; i.e., if the relative heat capacity of a PCM is stated to be four times that of concrete, then the implication is that a quantity of the PCM will perform equivalently to four times as much concrete.

Performance comparisons for PCM and concrete Trombe walls (Fig. 3) can be used to determine the validity of equivalent thicknesses and relative heat storage capacities. The results presented in Fig. 3 indicate that an approximate equivalence can be stated in some cases; e.g., curve E. In other cases, however, PCM solar fractions exceed the maximum solar fraction for the concrete Trombe wall, and a storage equivalence cannot be directly stated. It is nevertheless important to compare storage performance at equal solar fractions, and one way to achieve this is to use PCM and concrete walls with different aperture areas. Such storage and aperture trade-offs will be included in future SS PCM systems analyses.

4. CONFIGURATIONS FOR ENHANCED PCM PERFORMANCE

As described in the Sec. 3.3, performance for PCM Trombe walls improves as the phase transformation temperature is reduced to an optimum of approximately 27°C (80°F). To further maximize PCM performance, we now discuss alternative situations that allow lower phase transformation temperatures and reduced storage losses while maintaining adequate heat delivery rates. The objective is to minimize passive system standby losses and uncontrolled delivery of heat when it is not needed. The ideal system is analogous to an active system with well-insulated storage (and very high heat exchanger effectiveness between

storage and load). We discuss three alternative passive configurations, which if taken to ideal extremes, are essentially equivalent in terms of heat transfer. Some of these alternatives are more theoretical than practical, but serve to determine an upper bound for PCM performance and to identify what needs to be done to approach such idealized performance.

Note that an elevated phase transformation temperature causes not only increased heat losses but also increased sensible heat storage that to some extent offsets the heat losses. This offsetting effect is relatively large for the SS PCM analyzed here because of a high specific heat and relatively low enthalpy of transformation compared to other PCMs. For other PCMs, we expect the offsetting effect to be smaller and the benefits of a lower phase transformation temperature to be correspondingly greater. In the following discussion, we assume that the heat-loss effect is dominant and that a lower phase transformation temperature will result in a net benefit.

4.1 Trombe Wall

For the Trombe wall configuration, interior surface area equals aperture area, and heat delivery depends on the storage temperature and the heat-transfer coefficient at the interior surface. If this coefficient increases, then adequate heat delivery can be achieved even with a lower transition temperature, which, in turn, reduces heat losses from storage. The maximum benefit would occur if the heat-transfer coefficient were infinitely large and the transition temperature were equal to the heating setpoint. Then heat would be delivered from storage to the space only if there were a net heating load for the building (unless the latent heat capacity of the storage had been exceeded, in which case the storage temperature would be greater than the phase transformation temperature). This idealized PCM Trombe wall also assumes a high conductivity PCM so the interior surface temperature is not significantly lower than the phase transition temperature.

In practical cases, the surface heat-transfer coefficient can be increased somewhat by forced convection, but the potential for using lower phase transformation temperatures is not great. The concept is described here mainly as a vehicle for using Trombe wall results to indicate other configurations with high performance potential.

4.2 Direct Gain

For typical direct-gain configurations, storage within the building is charged during the day and delivers heat at night convectively to the room air and by long-wave radiation to other room surfaces. The heat delivery situation is similar to that for Trombe walls. Note, however, that even though storage surface area is typically larger in direct-gain systems, aperture losses are part of the heating load to be met by heat transfer from the storage surface area (while in a Trombe wall con-

figuration, heat is transferred from the exterior wall surface, and the room is effectively insulated from aperture losses). Further increases in storage surface area in a direct-gain system could allow for use of a lower phase-transformation temperature while still maintaining adequate heat delivery. The benefit would increase as the product of the surface area and the heat transfer coefficient increased and the phase transformation temperature approached the heating setpoint.

In practical cases, additional surface area may be available for storage, but it will be usable only if incoming solar energy can be adequately distributed. In typical direct-gain systems with storage charged primarily by direct beam solar radiation, storage-to-aperture ratios of between 3 and 6 are often assumed (9). Neepser and McFarland (10) have studied convectively charged PCM storage with area ratios between 6 and 12, and a phase-change temperature 1.6°C (3°F) above the heating setpoint. This low temperature was assumed to allow convective charging and discharging within the 5.5°C (10°F) thermostat deadband. The results were promising, but maximum performance for PCM storage was achieved only when the surface heat transfer coefficient was assumed to be three to four times larger than the normal values for natural convection.

4.3 Conductively Coupled Storage

In the previously described configurations, system optimization was limited by the need for phase-transformation temperatures above the heating setpoint except in hypothetical idealized cases. We now propose a configuration that avoids this limitation; i.e., a configuration in which heat delivery does not depend on a storage temperature above the heating setpoint. The proposed ideal configuration is one in which the PCM storage is in direct contact with building components through which heat is lost to ambient; e.g., a thin layer of PCM storage on the interior surfaces of exterior walls. The room air is buffered from heat losses by the presence of the PCM storage at the heating setpoint temperature.

In this configuration, heat delivery is by conduction to exterior building components, vis a vis typical passive solar configurations in which heat is delivered from storage to room air by convection. Hence, we refer to this configuration as conductively coupled storage. Note that the benefits of conductively coupled storage depend on the use of a PCM with a phase-transformation temperature at or near the heating setpoint; i.e., a sensible heat storage material that depends on elevated temperatures to store heat will not benefit from the conductively coupled storage configuration. Some portions of the building heating load (infiltration) are not amenable to the conductively coupled storage approach and would require some storage to be at an elevated temperature.

To the extent that PCM storage can be located as described and adequately charged, this configuration will approach ideal effectiveness for PCM

storage. Distribution of solar energy to a large storage area depends at least partially on convective charging, and a low phase-transformation temperature facilitates convective heat transfer. It may also be useful to employ aperture materials or devices that diffuse incoming solar radiation so it is dispersed widely over interior building surfaces.

4.4 Results

As an example of a configuration enhanced PCM performance, we simulated an idealized PCM Trombe wall with a transformation temperature of 20.3°C (68.5°F) and a surface heat-transfer coefficient of 567 W/m²°C (99.9 Btu/h ft²°F). The results for this case are presented as curve A in Fig. 3. Solar savings fractions for the idealized PCM Trombe wall are approximately 10%-20% higher than solar fractions for the optimized PCM Trombe wall with a typical heat-transfer coefficient (curve B).

The results presented as curve A in Fig. 3 for the idealized PCM Trombe wall are thought to represent an upper bound for the effectiveness of this particular PCM. Preliminary results for the conductively coupled storage configuration are similar to the results presented for the idealized Trombe wall.

5. CONCLUSIONS

Solid-state phase-change materials have certain advantageous characteristics, but effective use of these materials depends on an optimum combination of material properties and system design. Further improvements may be possible if materials research provides better SS PCMs.

PCM Trombe wall behavior is functionally different than the behavior of a concrete Trombe wall, resulting in different trends in material property sensitivities and PCM-to-concrete equivalences that are only valid for a specific set of circumstances.

For a typical Trombe wall configuration, performance is optimum for a PCM with high thermal conductivity and a phase transformation temperature that is a seasonal compromise between adequate heat delivery and storage heat loss.

In idealized passive configurations, the phase-transformation temperature equals the heating setpoint so storage losses are minimized and performance is maximized.

6. ACKNOWLEDGMENTS

I wish to thank David K. Benson, of SERI's Materials Research Branch for his guidance and support of this project and for his careful review of each stage of the work. This work was sponsored by the U.S. Department of Energy, Division of Passive and Hybrid Solar Heat Technologies.

7. REFERENCES

- (1) Bourdeau, Luc E. "Study of Two Passive Solar Systems Containing Phase-Change Materials for Thermal Storage," Proceedings of the 5th National Passive Solar Conference, American Solar Energy Society, Newark, DE, (1980).
- (2) Kohler, Joseph; Lewis, Daniel. "Phase-Change Products for Passive Homes," Solar Age, (June 1983), pp. 65-69.
- (3) Solomon, A. D. "Melt Time and Heat Flux for a Simple PCM Body," SOLAR ENERGY, 22, 251-257, (1979).
- (4) Solomon, A. D. "Design Criteria in PCM Wall Thermal Storage," ENERGY, 4, 701-709, (1979).
- (5) Hale, D. V., M. J. Hoover, and M. J. O'Neill. Phase-Change Materials Handbook, NASA Report MFS-22064, (Aug. 1972.) Available from NTIS.
- (6) Benson, D. K. et al. Materials Research for Passive Solar Systems: Solid-State Phase-Change Materials, SERI/TR-255-1828, Solar Energy Research Institute, Golden, CO, (1983), pg. 45.
- (7) Palmiter, L. and T. Wheeling. "SERIRES Version 1.0 User's Manual," Solar Energy Research Institute, Golden, CO, (forthcoming).
- (8) Hall, I. J., et al. "Generation of Typical Meteorological Years for 26 SOLMET Station," Proceedings of the 1978 Annual Meeting of AS/ISES, Vol. 2.2, American Section of the International Solar Energy Society, Newark, DE, (1978).
- (9) Balcomb, Douglas J., et al. Passive Solar Design Handbook, Volume Two, DOE/CS-0127/2, Los Alamos National Laboratory, Los Alamos, NM, (1980), pg. 270.
- (10) Neeper, Donald A.; McFarland, Robert. Some Potential Benefits of Fundamental Research for the Passive Solar Heating and Cooling of Buildings, LA-9425-MS, Los Alamos National Laboratory, Los Alamos, NM, (1982), pg. 43.